On the Chaperon Mechanism: Application to ClO + ClO (+N_2) → ClOOCl (+N_2)

Jingyao Liu[†] **and John R. Barker***

Department of Atmospheric, Oceanic, and Space Sciences, University of Michigan, Ann Arbor, Michigan 48109-2143

Received: April 17, 2007; In Final Form: June 19, 2007

The dynamics of the ClO + ClO (+N_2) radical complex (or chaperon) mechanism is studied by electronic structure methods and quasi-classical trajectory calculations. The geometries and frequencies of the stationary points on the potential energy surface (PES) are optimized at the B3LYP/6-311+G(3df) level of theory, and the energies are refined at the CCSD(T)/6-311+G(3df) (single-point) level of theory. Basis set superposition error (BSSE) corrections are applied to obtain 1.5 kcal mol^{-1} for the binding energy of the ClO·N_2 van der Waals (VDW) complex. A model PES is developed and used in quasi-classical trajectory calculations to obtain the capture rate constant and nascent energy distributions of ClOOCl* produced via the chaperon mechanism. A range of VDW binding energies from 1.5 to 9.0 kcal mol^{-1} are investigated. The anisotropic PES for the ClO·N_2 complex and a separable anharmonic oscillator approximation are used to estimate the equilibrium constant for formation of the VDW complex. Rate constants, branching ratios to produce ClOOCl, and nascent energy distributions of excited ClOOCl* are discussed with respect to the VDW binding energy and temperature. Interestingly, even for weak VDW binding energies, the N_2 usually carries away enough energy to stabilize the nascent ClOOCl*, although the VDW equilibrium constant is small. For stronger binding energies, the stabilization efficiency is reduced, but the capture rate constant is increased commensurately. The resulting rate constants for forming ClOOCl* from the title reaction are only weakly dependent on the VDW binding energy and temperature. As a result, the relative importance of the chaperon mechanism is mostly dependent on the VDW equilibrium constant. For the calculated ClO·N_2 binding energy of 1.5 kcal mol^{-1}, the VDW equilibrium constant is small, and the chaperon mechanism is only important at very high pressures.

I. Introduction

An exothermic radical + radical recombination reaction produces an excited product with enough energy to redissociate. In order to obtain a stable product, the energy must be removed. In the limit of zero pressure, energy may be lost by spontaneous infrared emission, resulting in stabilized product molecules,[1] but at higher pressures, interactions with the bath gas are dominant in producing a stabilized product.[2] Historically, two mechanisms have been invoked to explain the pressure dependence of recombination (and unimolecular dissociation) reactions.[3] For larger free radicals at low to moderate densities, the energy transfer (ETM), or Lindemann, mechanism[2] is probably most important

$$A + B \rightleftharpoons C^* \qquad (R1,-R1)$$

$$C^* + M \rightarrow C + M \qquad (R2)$$

where A and B are reactants, C is the product, the asterisk denotes internal excitation, and M is an energy transfer collider. When the concentration of C* is in a pseudosteady state, the effective second-order rate constant for recombination of A and B to produce stabilized C depends on the concentration of M

$$k_{ETM} = \frac{k_1 k_2[M]}{k_{-1} + k_2[M]} \qquad (E1)$$

where the square brackets denote concentration. This equation is the basis for the strong collision and master equation versions of the Rice−Ramsperger−Kassell−Marcus (RRKM) Theory.[4−8]

At higher densities, lower temperatures (such as in earth and planetary atmospheres), and for smaller reactant species, a second mechanism may become important, the radical complex (RCM), or chaperon, mechanism.[9] For present purposes, we include in this category any reaction in which a chaperon is involved, including chemical activation systems initiated by a recombination step. For example, the well-known acceleration of the HO_2 + HO_2 reaction by water vapor[10−15] is an example of the RCM. Other examples are known from high-pressure experiments.[3,16−18] The RCM entails formation of a weakly bound radical, or van der Waals (VDW), complex, which subsequently reacts with a second reactant to produce the recombination product

$$A + M \rightleftharpoons A{\cdot}M^* \qquad (R3,-R3)$$

$$A{\cdot}M^* + M \rightarrow A{\cdot}M + M \qquad (R4)$$

$$A{\cdot}M + B \rightarrow C{\cdot}M^* \qquad (R5)$$

$$C{\cdot}M^* \rightarrow C^* + M \qquad (R6)$$

Here, A·M is the weakly bound VDW complex, and the asterisk denotes internal excitation. According to the usual chaperon

* To whom correspondence should be addressed. E-mail: jrbarker@umich.edu.

[†] Permanent address: Institute of Theoretical Chemistry, State Key Laboratory of Theoretical and Computational Chemistry, Jilin University, Changchun 130023, People's Republic of China.

10.1021/jp072978p CCC: $37.00
Published on Web 08/14/2007

model, it is assumed that the vibrationally excited C* produced in reactions R5 and R6 does not have enough energy to dissociate back to A + B. An analogous B·M complex may also be formed and may react in a similar manner. According to this mechanism, if [M] is much greater than the other concentrations, then the net rates of reactions R3 and R4 will be much faster than that of reaction R5 and fast enough to maintain the net equilibrium

$$A + M \rightleftharpoons A\cdot M \qquad \text{(R7)}$$

with equilibrium constant K_{VDW}. The resulting recombination rate constant has the same functional form as k_{ETM}, although the factors are different in magnitude and depend more sensitively on temperature and the nature of the collider gas[3,17,19,20]

$$k_{RCM} = \frac{K_7 k_6[M]}{1 + K_7[M]} \qquad \text{(E2)}$$

Generally speaking, the ETM is used in the conventional analysis of recombination rate data.[12,21] If the ETM analysis fails in some way, the RCM is often implicated by default. Quantitative assessment of the ETM is relatively routine because widely available master equation codes are all based on the ETM[22] (for example, see the MultiWell Program Suite[23,24]). The same is not true of the RCM.

The ClO + ClO recombination reaction exhibits anomalous energy transfer rates and temperature dependence.[3,25] This ClO self-reaction has attracted considerable attention experimentally[26−31] and theoretically[32−41] because of the key role of the "ClO dimer" (ClOOCl) in the ozone destruction cycle that takes place in the polar stratospheric ozone hole. Experimental studies have observed that the rate constant near the low-pressure limit is larger than that predicted by standard RRKM treatments.[3,25] It has been suggested that the chaperon mechanism may play a significant role in this system,[3,18,29,42−44] even though the ClO·N_2 van der Waals binding energy is not expected to be very large. Because of the potential importance of N_2 as a chaperone in atmospheric reactions and because the number of electrons in the ClOOCl·N_2 systems is not too large for reasonably high levels of electronic structure theory, it is a good system for investigating the fundamental dynamics of the RCM.

The present Article is our first step toward a systematic implementation of the RCM in master equation simulations. Our ultimate aim is a quantitative description of the RCM. To achieve this goal, a quantitative assessment of the equilibrium constant for reaction R7 and knowledge of the nascent energy distribution of product C produced in reaction R6 are required. Quantitative analysis of the equilibrium constant has been addressed by several research groups.[9,45−50] To the best of our knowledge, however, the energy distributions have never been considered quantitatively with the aim of incorporating them in a master equation analysis, which is the aim of the present work.

The nascent energy distribution of C produced in reaction R6 is important for two reasons. First, the energy distribution is directly related to the overall rate of production of stabilized C. If the energy distribution does not extend significantly above the reaction threshold energy, then redissociation of C will be unimportant. Conversely, if the energy distribution of C is located substantially above the threshold energy for dissociation, then little stabilized C will be produced at low pressures. In all previous kinetics applications of the RCM, it has been implicitly assumed that C from reaction R6 is completely stabilized. This assumption was not needed in the pioneering trajectory calculations on the RCM carried out by Varandas et al.,[51] who, however, did not report the calculated nascent energy distributions.

The second reason that the nascent energy distribution is needed for initializing master equation calculations is because it controls the product distribution when multiple reaction channels are present. This is a common occurrence. For example, the ClO + ClO recombination reaction is but the first step in a more complex mechanism, which arises, in part, from the several reaction pathways open to excited ClOOCl*. The product yields depend on the nascent energy distribution of excited ClOOCl* and on the reaction thresholds[41] of the reaction channels

$$\text{ClOOCl*} \rightarrow \text{ClO} + \text{ClO} \qquad \text{(R8a)}$$
$$\rightarrow \text{Cl}_2 + \text{O}_2 \qquad \text{(R8b)}$$
$$\rightarrow \text{Cl} + \text{ClOO} \qquad \text{(R8c)}$$
$$\rightarrow \text{ClOClO*} \qquad \text{(R8d)}$$
$$\rightarrow \text{etc.}$$

When ClOOCl* is produced via the ETM, its nascent energy distribution is different than that when it is produced via the RCM. A master equation analysis enables calculation of reaction branching ratios as experimental pressures and temperatures are varied.[22]

In this Article, we use a model potential energy surface (PES) and quasi-classical trajectory calculations to investigate the nascent energy distributions of ClOOCl* produced via reactions R1 and R6. Here, N_2 is the energy transfer collision partner. The model PES is intended to be of sufficient accuracy to draw conclusions about the nascent energy distributions but not necessarily sufficiently accurate to simulate actual experiments. In future work, we will use knowledge of the nascent energy distributions to construct a master equation model suitable for simulating experiments.

II. Theoretical Methods

In this work, quantum chemical calculations are performed to obtain the potential energy surface information using the Gaussian 98 program.[52] The molecular dynamics program VENUS96[53] was employed to obtain the capture rate constant and the energy distribution by the quasi-classical trajectory calculations. In VENUS96, the potential energy is first formulated in terms of curvilinear internal coordinates and then transformed to Cartesian coordinates. With this procedure, the accuracy of the Hamiltonian depends only on the potential energy since no terms are neglected in the kinetic energy expression.[54]

A. Potential Energy Surface. The multidimensional potential energy surfaces for ClOOCl and ClOOClN_2 are constructed with a many-body expansion approach. The Morse oscillator is used to model the bond stretches, and the harmonic approximation is used to model the bond bending. Potential energy functions V_1 and V_2 are used to describe ClOOCl and ClOOClN_2, respectively

$$V_1 = \sum_{i=1}^{2} D_{ClO}[1 - e^{-\beta_{ClO}(r_{ClO} - r^0_{ClO})}]^2 + \sum_{i=1}^{1} D_{OO}[1 - e^{-\beta_{OO}(r_{OO} - r^0_{OO})}]^2 + \sum_{i=1}^{2} \frac{1}{2} f_{ClOO} S(r_{ClO}) S(r_{OO}) (\theta^i_{ClOO} - \theta^0_{ClOO})^2 + \sum_{n=1}^{2} \frac{1}{2} k^n_d S(r_1)[1 + \cos(n\tau - \gamma_n)] + \sum_{i=1}^{2} f_{ClO-OO}(r^i_{ClO} - r^0_{ClO})(r_{OO} - r^0_{OO}) + \sum_{i=1}^{1} f_{ClO-ClO}(r^i_{ClO} - r^0_{ClO})(r_{ClO} - r^0_{ClO}) \quad \text{(E3)}$$

and

$$V_2 = V_1 + \sum_{i=1}^{4} D_{ClN}[1 - e^{-\beta_{ClN}(r^i_{ClN} - r^0_{ClN})}]^2 + \sum_{i=1}^{1} D_{NN}[1 - e^{-\beta_{NN}(r_{NN} - r^0_{NN})}]^2 + \sum_{i=1}^{4} \frac{1}{2} f_{OClN} S(r_{ClO}) S(r_{ClN}) (\theta^i_{OClN} - \theta^0_{OClN})^2 + \sum_{i=1}^{4} \frac{1}{2} f_{ClNN} S(r_{ClN}) S(r_{NN}) (\theta^i_{ClNN} - \theta^0_{ClNN})^2 + \sum_{i=1}^{1} f_{ClO-NN}(r^i_{ClO} - r^0_{ClO})(r_{NN} - r^0_{NN}) \quad \text{(E4)}$$

In eq E3, ClOOCl is described with three Morse stretches (the first two terms), two harmonic bends (the third term), one dihedral angle (the fourth term), and three nondiagonal stretch−stretch interaction terms (the fifth term). In eq E4, $ClOOClN_2$ is represented by starting with the potential functions for ClOOCl and adding Morse oscillators for the N−N and Cl−N bond stretches, harmonic oscillators for the O−Cl−N and Cl−N−N bends, and nondiagonal stretch−stretch interactions between the Cl−O and N−N bond stretches. In eqs E3 and E4, the D_{ij} terms are the bond dissociation energies, β_{ij} are the Morse exponential terms, r_{ij} are the bond lengths, θ_{ijk} are the bond angles, and k^n_d is the contribution of the potential barrier to internal rotation that depends on dihedral angle τ with periodicity n. Switching functions are used to attenuate or modify force constants of bending and torsional modes as the molecule undergoes bond fission. The nondiagonal force constants f_{ij-kl} are defined by

$$f_{ij-kl} = f^0_{ij-kl}\, S(r_{ij}) S(r_{kl}) \quad \text{(E5)}$$

where $S(r_i)$ are switching functions (attenuation terms) given by

$$S(r_{ij}) = \exp[-C_{ij}(r_{ij} - r^0_{ij})] \quad \text{(E6)}$$

where C_{ij} is an attenuation parameter ($C_{ij} \geq 0$).

Initial estimates for the dissociation energies, torsion barrier heights, and attenuation parameters in the harmonic bends are from the quantum chemical calculations. The optimized geometries of the stationary points on the PES are obtained using the hybrid density functional B3LYP method, that is, Becke's three-parameter nonlocal exchange functional[55] with the nonlocal correlation functional of Lee, Yang, and Parr[56] with the 6-311+G(3df) basis set (B3LYP/6-311+G(3df)). In order to obtain more accurate energetic information, single-point energy calculations are performed at the CCSD(T) level of theory (coupled−cluster approach with single and double substitutions including a perturbative estimate of connected triples substitutions) with the same basis set (CCSD(T)/6-311++G(3df)), as well as at the G3(MP2) theory[57] at the B3LYP/6-311+G(3df) geometries. In addition, the calculations for the $ClO{\cdot}N_2$ complex are performed at the CCSD(T)/6-311++G(3df)//MP2/6-311+G(3df) and CCSD(T)/ 6-311++G(3df)//CCSD/6-311+G(2df) levels to improve the accuracy of the binding energy. All electronic calculations are performed by using the Gaussian 98 program.[52]

TABLE 1: Potential Energy Surface Parameters

parameter	value	parameter	value
D_{ClO}	20.83 kcal/mol	β_{ClO}	2.832 Å^{-1}
D_{OO}	18.66 kcal/mol	β_{OO}	2.802 Å^{-1}
D_{ClN}	0.9 kcal/mol	β_{ClN}	1.011 Å^{-1}
D_{NN}	218.20 kcal/mol	β_{NN}	2.86 Å^{-1}
r^0_{ClO}	1.7481 Å	f_{ClOO}	1.2 mdyn Å/rad^2
r^0_{OO}	1.361 Å	f_{OClN}	0.05 mdyn Å/rad^2
r^0_{ClN}	3.2195 Å	f_{ClNN}	0.0005 mdyn Å/rad^2
r^0_{NN}	1.0909 Å	f^0_{ClO-OO}	0.5924 mdyn/Å
θ^0_{ClOO}	111.40°	f^0_{ClO-OO}	−0.0052 mdyn/Å
θ^0_{OClN}	179.7°	f^0_{ClO-NN}	0.2479 mdyn/Å
θ^0_{ClNN}	178.1°		

B. Capture Rate Constant. The quasi-classical trajectory method is used to obtain capture rate constants by using the standard expression[58,59]

$$k_{cap}(T) = g_e(T)\left(\frac{8k_BT}{\pi\mu}\right)^{1/2} \pi b^2_{max}\left(\frac{N_r}{N}\right) \quad \text{(E7)}$$

where μ is the reduced mass of the reactants, N_r is the number of trajectories that form a capture complex, N is the total number of trajectories in the ensemble, b_{max} is the maximum impact parameter, and the electronic degeneracy factor assumes the form

$$g_e(T) = \frac{1}{[(2 + 2\exp(-E_1/RT)]^2} \quad \text{(E8)}$$

where $E_1 = 320.3$ cm^{-1} is the energy difference between $ClO(X^2\Pi_{1/2})$ and $ClO(X^2\Pi_{3/2})$.[60] The collision impact parameter b is chosen by VENUS96 according to

$$b = b_{max} R^{1/2} \quad \text{(E9)}$$

where R is a (pseudo-) random number distributed uniformly between 0 and 1. The maximum impact parameter b_{max} is determined empirically in order to include ≥95% of the complex-forming trajectories.

TABLE 2: Vibrational Frequencies (cm^{-1}) and Moments of Inertia at the Stationary Points

	B3LYP/6-311+ G(3df)	PES for quasi-classical trajectories	experimental	moments of inertia[a]
ClO	861		854	27.038(2)
N_2	2446		2359	8.437(2)
$ClO{\cdot}N_2$	28,45,62,71,861, 2449			0.0425(1), 370.2(2)
ClOOCl	126,326,442,549, 636,845	123,336,402,560, 658,731	127,321,419,543, 648,754 (ref 79)	37.58(1), 236.6(2)
$ClOOCl{\cdot}N_2$	12,25,38,61,68,129,328, 442,551,637,842,2449	3,13,35,47,56,129,338, 404,560,659,731,2453		93.08(1), 829(2)

[a] Moments of inertia expressed in units of amu $Å^2$. Rotor dimensions are in parentheses; nonlinear molecules are approximated as symmetric tops with a 1-dimensional rotor (the K-rotor) and a 2-dimensional rotor; linear molecules have only a 2-dimensional rotor.

In this work, batches of 10^4-10^5 trajectories are used to determine the capture number N_r. Trajectories are averaged over vibrational phases and integrated for 2×10^6 time steps with a step size of 0.1 fs. Initial conditions are selected randomly by using the standard options in VENUS96.[53] As in other work from this laboratory,[59,61−63] the initial relative translational energies of the reactants are chosen randomly from thermal distributions by using Monte Carlo selection techniques. For the purpose of selecting the initial energy distributions, rotational and vibrational degrees of freedom are assumed to be approximately separable. Polyatomic molecule initial vibrational energies are selected from a Boltzmann distribution of normal mode energies. Diatomic molecule initial energies are selected according to $v = 0$ (vibrational quantum number) and J (total angular momentum quantum number). In some series of calculations, J is varied over a range of values. In other calculations, J is set at the most probable value for a given temperature.

As discussed in previous work on the OH + NO_2 reaction,[59] there are several possible criteria for determining whether capture has taken place. These criteria may be based on center of mass distances and/or on the number of turning points resulting from multiple vibrational periods of the newly formed bond. The choice of the criteria is arbitrary. Fortunately, experience with this and with the OH + NO_2 reaction indicates that the results are not very sensitive to a particular choice. In the present work, we counted a trajectory as resulting in capture when the number of turning points equaled or exceeded 15.

III. Results and Discussion

A. Electronic Structure Calculations. The geometries of the stationary points on the PESs for the ETM and the RCM are optimized at the B3LYP/6-311+G(3df) level of theory. For the RCM, two weakly bound van der Waals (VDW) complexes ($ClO{\cdot}N_2$ and $ClOOCl{\cdot}N_2$) are located and optimized. Vibrational frequency analysis at each VDW minimum yields only positive frequencies, thus ensuring that the structures are true local minima on the PES. For comparison, the structures of ClOOCl and the $ClO{\cdot}N_2$ VDW complex are optimized at the MP2/6-311+G(3df) and CCSD/6-311+G(2df) levels. The higher level energies are calculated at the CCSD(T)/6-311+G(3df) and the G3(MP2) levels of theory. The optimized geometries and frequencies of the stationary points are shown in Figure 1 and Table 2, respectively, along with the available experimental data.[60] The ClOOCl structure is found to have C_2 symmetry (like hydrogen peroxide), and its geometric parameters obtained at these levels of theory are in reasonable agreement with the experimental values.[60] The largest discrepancy is observed for the O−O bond distance; the calculated value is about 0.055 Å shorter than the value given in NIST-JANAF.[60] The theoretical and experimental[26,29,64,65] dissociation energies D_0(ClOOCl) for ClOOCl → ClO + ClO are compared in Table 3. It is seen that good agreement is obtained between the single-point energies calculated with the B3LYP and MP2 geometries. The value for D_0(ClOOCl) calculated using CCSD(T)//B3LYP is in better agreement with the latest experimental result[64,65] and was used with zero-point energy (ZPE) corrections to parametrize the PES.

The two VDW complexes $ClO{\cdot}N_2$ and $ClOOCl{\cdot}N_2$ have Cl−N equilibrium bond distances of 3.2658 and 3.2195 Å, respectively, at the B3LYP/6-311+G(3df) level of theory. The intramolecular Cl−N distance in $ClO{\cdot}N_2$ calculated by B3LYP theory is in good agreement with the CCSD value, and both are slightly longer than the MP2 result. As can be seen in Table 2, the ClO and N_2 stretching mode frequencies of the complex are very similar to the Cl−O and N−N stretching frequencies of the isolated ClO radical and N_2 molecule. The $ClO{\cdot}N_2$ VDW binding energy (ϵ_1^0) is calculated to be 1.12, 1.13, and 1.18 kcal mol^{-1} (including ZPE) at the CCSD(T)//B3LYP, CCSD(T)//CCSD, and CCSD(T)//MP2 levels of theory, respectively.

It is known that for the weakly bound compounds, such as VDW and hydrogen-bonded complexes, the basis set superposition error (BSSE) is of the same order of magnitude as the binding energies themselves; thus, the BSSE is especially important in these systems. The BSSE correction for the $ClO{\cdot}N_2$ complex is calculated in two ways, by the counterpoise (CP) scheme of Boys and Bernardi[66] and by the CBS-QB3 complete basis set extrapolation method.[67,68] The energy results are listed in Table 3. The uncorrected CCSD(T)//B3LYP (CCSD(T)//CCSD or CCSD(T)//MP2) binding energy is very nearly equal to the CBS-QB3 value (0.96 kcal mol^{-1}), while the CP-corrected binding energy is slightly lower. This may indicate that the CP method overestimates the BSSE, as sometimes happens.[69−73] Thus, we conclude that the B3LYP geometries and uncorrected CCSD(T)//B3LYP binding energy for the O−Cl···N−N complex (ϵ_1^0 = 1.12 kcal mol^{-1} including ZPE corrections; 1.57 kcal mol^{-1} without ZPE corrections) are reasonably accurate and are used later to estimate the equilibrium constant for van der Waals dimer formation. The VDW binding energies (ϵ_2^0) calculated for $ClOOCl{\cdot}N_2$ agree with those for $ClO{\cdot}N_2$ within ~0.1 kcal mol^{-1}.

Since one of our main goals in this work is to obtain insight into the generic RCM, we consider model VDW binding energies of ϵ_2 = 1.5, 3.0, 4.5, and 9.0 kcal mol^{-1}. This enables us to determine the contributions of the RCM to the overall rate coefficient for a wide range of possible VDW complexes. The effects of these binding energies on the equilibrium constant for reaction R7 and on the nascent energy distribution of excited ClOOCl* are determined. The analytic PES assumes that $\epsilon_1 = \epsilon_2$, and thus, the subscript is omitted in the discussion below unless it is needed for clarity.

B. Equilibrium Constant. In order to obtain the rate constant k_{RCM} as a function of pressure, it is necessary to evaluate the

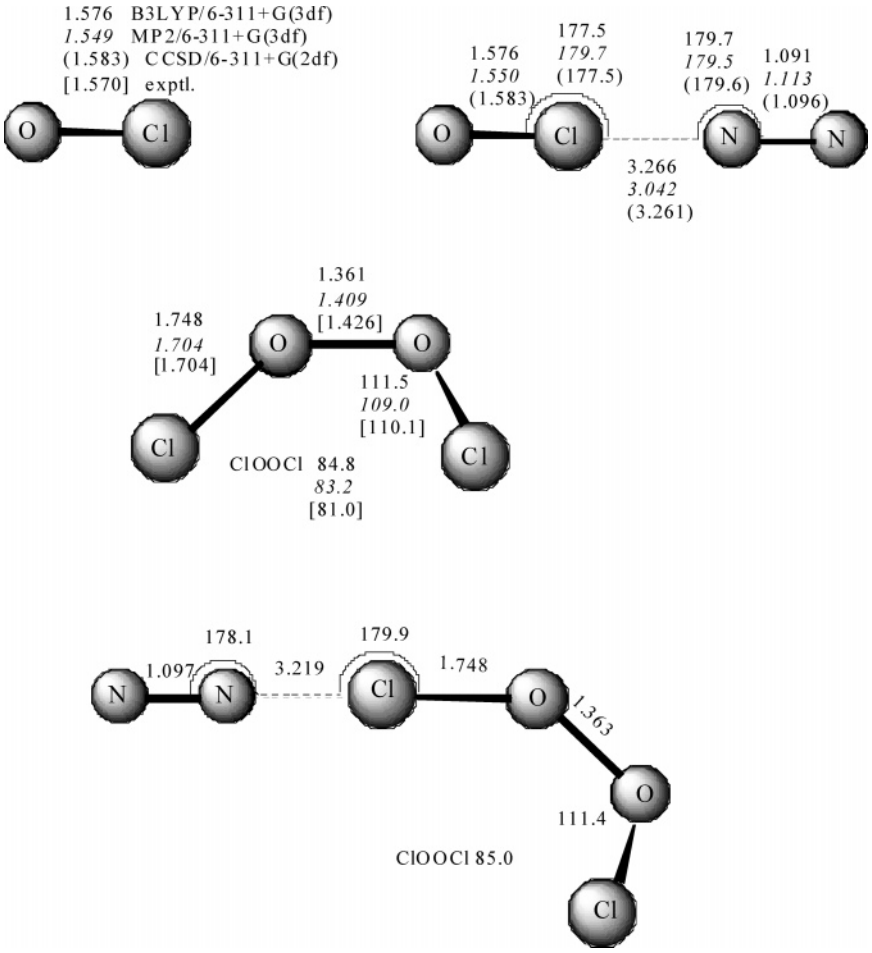

Figure 1. Molecular species and structural parameters calculated at various levels of theory.

TABLE 3: Dissociation Energies (in kcal/mol) with ZPE Corrections

	D_0 (ClO−OCl)	D_{0M} (ClO−OClN$_2$)	ϵ_1^0 (ClO−N$_2$)	ϵ_2^0 (ClOOCl−N$_2$)
B3LYP/6-311+G(3df)	11.81	11.76	0.22	0.17
CCSD(T)/6-311+G(3df)//B3LYP	16.93[a]	16.93[a]	1.12[b]	1.22[a]
G3(MP2)//B3LYP	19.02	19.15	0.99	1.11
MP2/6-311+G(3df)	31.94		1.27	
CCSD(T) /6-311+G(3df)//MP2	17.54		1.18	
G3(MP2)//MP2	19.67		0.88	
CCSD(T)/6-311+G(3df) //CCSD/6-311+G(2df)			1.13	
CP[c]-CCSD(T)/6-311+G(3df) //B3LYP			0.62	
CBS-QB3			0.96	
experimental		16.5 ± 0.7,[d] 18.6 ± 0.7,[e] 16.3 ± 0.7,[f] 15.9 ± 0.7[g]		

[a] Used with ZPE corrections to assign D_e in the PESs. [b] Used in the calculation of K_{VDW}. [c] Counterpoise corrected energy. [d] Ref 26. [e] Ref 29. [f] Ref 64. [g] Ref 65.

equilibrium constant for forming a VDW complex (reaction R7). The equilibrium constant can be written

$$K_{VDW} = \frac{Q^{\circ}_{complex}}{Q^{\circ}_{ClO}\, Q^{\circ}_{N_2}} \exp\left(\frac{\epsilon_1^0}{k_b T}\right) \qquad \text{(E10)}$$

where Q_i^0 (referenced to the ZPE of the ith species) is the total partition function per unit volume and ϵ_1^0 is the VDW binding energy (corrected for ZPE) that corresponds to VDW well depth ϵ_1 (not corrected for ZPE). For the nominal value $\epsilon_1 = 1.5$ kcal mol^{-1}, we use $\epsilon_1^0 = 1.12$ kcal mol^{-1}, which is the best estimate of the actual ClO−N_2 binding energy (see Table 2 and discussion above). For the remaining three assumed binding energies ($\epsilon_1 = 3.0$, 4.5, and 9.0 kcal mol^{-1}), we assume the ZPE difference is approximately 0.4 kcal mol^{-1}, giving $\epsilon_1^0 =$ 2.6, 4.1, and 8.6 kcal mol^{-1}, respectively. The translational, vibrational, rotational, and electronic partition functions are calculated by Thermo[23,24] using standard statistical mechanics formulas. Since the harmonic oscillator is a poor description of the low-frequency VDW bond, which can dissociate, the

TABLE 4: Equilibrium Constants (K_{VDW})[a]

	VDW well depth ϵ[b]			
T(K)	1.5[c]	3.0	4.5	9.0
200	2.71(−23)	1.15(−21)	5.01(−20)	4.12(−15)
300	1.71(−23)	2.08(−22)	2.58(−21)	4.88(−18)
400	1.53(−23)	9.95(−23)	6.58(−22)	1.89(−19)
500	1.51(−23)	6.77(−23)	3.07(−22)	2.84(−20)

[a] Units: cm^{-3} molecule; estimated accuracy: $\sim\times 10^{\pm 1}$. [b] Well depth ϵ in units of kcal mol^{-1} (no ZPE corrections). [c] Note that $\epsilon = 1.5$ kcal mol^{-1} is predicted in Table 3 to be most accurate for $ClO{\cdot}N_2$.

anharmonic oscillator approximation is used instead. The anharmonicity constants are calculated by assuming the VDW bond is described by a Morse oscillator potential function. This is only an approximation to the VDW potential energy function, but it at least includes the ability to dissociate, which is totally missing from the harmonic oscillator approximation.

The VDW equilibrium constants K_{VDW} calculated using the anharmonic oscillator and anisotropic potential are presented in Table 4 for three temperatures and four assumed VDW binding energies (note that our ab initio calculations in Table 2 predict that $\epsilon_1 = 1.5$ kcal mol^{-1}). Although the numerical values for K_{VDW} are given with three significant digits, they are probably only accurate to about an order of magnitude. More accurate numerical values can be obtained by using hindered rotor potential energy functions in place of the harmonic potentials used for the bending modes. Furthermore, the degrees of freedom are probably not separable. Varandas and co-workers[48−50] have shown how Monte Carlo integration of the classical phase space integral can be used to calculate the partition function for nonseparable potentials. Such methods are needed for more accurate predictions of K_{VDW}. The approximate values in Table 4 are sufficient for the present order-of-magnitude estimates, however.

Although the ab initio calculations predict $ClO{\cdot}N_2$ to be nonlinear, the deviation from linearity is small. If we assume the VDW complex is exactly linear, there is no K-rotor, and one bending vibrational mode becomes doubly degenerate. Calculations assuming the doubly degenerate bending mode has a frequency in the range of 62−71 cm^{-1} give K_{VDW} values that are 3 times those shown in Table 4, which is within the order-of-magnitude accuracy estimated for K_{VDW}.

The equilibrium constant K_{VDW} is often estimated by using the Bunker−Davidson relationship[9] and Stogryn−Hirschfelder[45] method. In the latter approximation, metastable states with energies larger than the binding energy but smaller than the centrifugal barriers of the VDW complexes are included. Similar calculations for the equilibrium constant have been carried out by Luther, Troe, and co-workers,[17,74] based on work by Schwarzer and Teubner.[46] It is interesting to compare these methods, which were designed for atom + atom recombination reactions, to the anharmonic oscillator model described in the preceding paragraph. Both of the atom + atom methods assume that the potential energy function is isotropic with respect to both partners. According to our calculations, however, significant VDW wells are located only in the vicinity of the Cl atoms. Furthermore, the N_2 bond is essentially collinear with the ClO bond. Thus, the potentials are quite anisotropic. The anisotropy is represented in the anharmonic oscillator model by bending and torsional potential energy functions, which reduce the available phase space and hence reduce the calculated equilibrium constants.

Lennard-Jones parameters ($\sigma_{LJ} = 3.8385$ Å and $\epsilon_1/k_B = 754.9$ K) for $ClO + N_2$ were obtained by using the $OCl{\cdot}N_2$ equilibrium distance r_e from the B3LYP/6-311+G(3df) geometry optimization ($\sigma_{LJ} = 2^{-1/6}r_e$) and the VDW binding energy from the CCSD(T)/6-311+G(3df)//B3LYP calculation. The Bunker−Davidson method gives $K_{VDW} = 3.93 \times 10^{-21}$, 1.78×10^{-21}, and 6.95×10^{-22} cm^3 $molecule^{-1}$ at 200, 300, and 500 K, respectively, which are slightly lower than those obtained using the Stogryn−Hirschfelder method at the same temperatures, 5.66×10^{-21}, 2.84×10^{-21}, and 9.87×10^{-22} cm^3 $molecule^{-1}$. Equilibrium constants obtained at the same three temperatures using the anharmonic oscillator approximation with the anisotropic PES (Table 4, 2.71×10^{-23}, 1.71×10^{-23}, and 1.51×10^{-23} cm^3 $molecule^{-1}$) are only a few percent of those calculated using the Bunker−Davidson and Stogryn−Hirschfelder methods, showing the important reduction in available phase space volume due to anisotropy.

In his Ph.D. Thesis, Harald Stark reported measurements of the rate constant for the ClO + ClO reaction in He and N_2 bath gases at 200 and 300 K for pressures ranging from ∼0.1 to ∼1000 bar.[18] Although his results have not been published in the peer-reviewed literature, they have been cited as providing strong support for the RCM.[3,44] Stark analyzed his data by combining the effects of diffusion, the ETM, and the RCM. As part of his analysis, he used the Bunker−Davidson relationship[9] and, by estimation and curve fitting, arrived at values for the Lennard-Jones parameters for $Cl{\cdot}N_2$, $\sigma_{LJ} = 4.4$ Å and $\epsilon_1/k_B = 331$ K (errors are not stated). These values, which are similar to those found in the present work, give values for the equilibrium constant that are within a factor of 3 of those found above using the Bunker−Davidson method. However, the Bunker−Davidson method neglects anisotropy of the potential energy surface. Equilibrium constants obtained in the present work with the anisotropic PES (Table 4) have a weaker temperature dependence and are about 1/30th of the magnitude.

C. Quasi-Classical Trajectory Calculation. Consider the following reactions and the vibrationally excited species that result from them

$$ClO + ClO \rightarrow ClOOCl^* \quad \text{(R9)}$$

$$ClO + ClO{\cdot}N_2 \rightarrow ClOOCl{\cdot}N_2^* \quad \text{(R10)}$$

$$ClOOCl{\cdot}N_2^* \rightarrow ClOOCl^* + N_2 \quad \text{(R11)}$$

Batches of 10^4−10^5 trajectories are used to perform quasi-classical trajectory calculations to obtain the capture rate constant for reactions R9 and R10 at 200, 300, and 500 K and to investigate the nascent energy distributions of ClOOCl* produced via reactions R9 and R11 based on the model PES constructed above. By varying parameter D_{ClN} in eq E4, the VDW well depth is adjustable in the model PES. Trajectories are averaged over phases and integrated with a step size of 0.1 fs. The initial rotational and relative translational energies of the reactants are chosen randomly from thermal distributions. Initial conditions for the vibrations of polyatomics were selected using microcanonical normal mode sampling. The initial vibrational energy of ClO radicals was selected semiclassically for $v = 0$. All of the sampling of initial conditions was carried out by using the standard features in VENUS96.[53]

The nascent energy distributions obtained by binning the quasi-classical trajectory calculation results are shown in Figure 2. The nascent energy distribution of ClOOCl* produced in reaction R9 is, by definition, located entirely above the threshold energy for dissociation, which is equal to the quantity ($D_e + 2 \times ZPE_{ClO}$). The quasi-classical method includes the zero-point energy of each ClO radical (ZPE_{ClO}) when randomly selecting

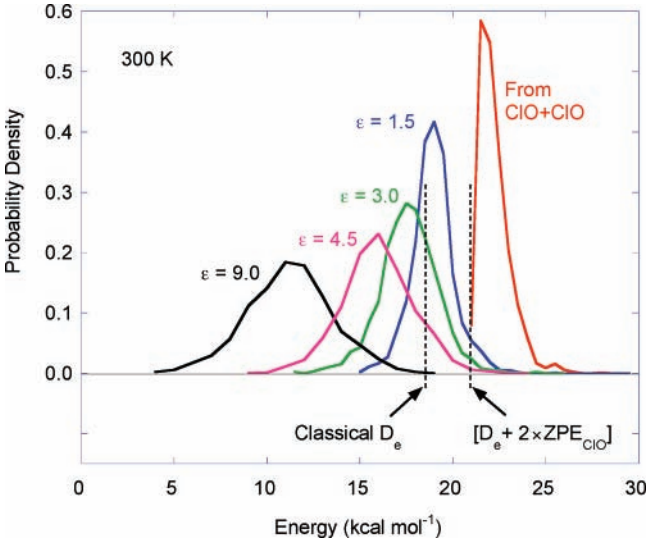

Figure 2. Nascent energy distributions of the excited ClOOCl* produced in the ClO + ClO and in the ClO + ClO·N_2 reactions. VDW well depths (ϵ, kcal mol^{-1}) are with no ZPE corrections. Also shown are the classical bond dissociation energy (D_e) and the energy threshold ($D_e + 2 \times ZPE_{ClO}$) used to initialize the quasi-classical trajectory calculations.

initial energies, and the resulting initial energy distribution is in excellent quantitative agreement with the chemical activation distribution function,[4,5,7] which is used in master equation simulations of recombination reactions.[22,23]

Because the entire chemical activation energy distribution of ClOOCl* produced from the ClO + ClO reaction is above D_0, all of the ClOOCl* will redissociate unless collisionally stabilized. The corresponding energy distribution of ClOOCl* produced from the ClO·N_2 + ClO reaction is at a lower energy and not as sharply peaked as the chemical activation distribution. It shifts toward still lower energies as the VDW well becomes deeper. Thus, the probability for forming stable ClOOCl increases as the well deepens. Even for VDW well depths as small as $\epsilon = 1.5$ kcal mol^{-1} (without ZPE corrections), collision-free redissociation of ClOOCl* is very minor because almost all of the nascent energy distribution falls below D_0 (classically, of course, much more ClOOCl* would dissociate). This result supports the usual assumption that the RCM produces stabilized products.

The energy distributions of ClOOCl* produced from the ClO·N_2 + ClO reaction are also in good qualitative agreement with experimental[75−77] and calculated[61] distributions of the translational recoil energy that is released when an excited VDW complex dissociates. The energy distributions both in the previous work and in the present work show that some of the excitation energy is used to break the VDW bond, and most of the remainder remains as excitation in the product molecule. Very little energy remains to be distributed among the rotational and translational degrees of freedom. A classical physical model that explains this behavior[61] is based on the fact that the VDW modes (one bond stretch, three bends, and one torsion for ClOOCl·N_2) have very low frequencies and therefore are coupled only very weakly to the much higher frequency internal vibrations of ClOOCl and N_2. Because of the weak coupling, the rate of energy transfer from excited ClOOCl* to the VDW modes is much slower than the rate of dissociation of the VDW bond, just above the dissociation threshold. Therefore, dissociation occurs as soon as just enough energy has been transferred to break the bond and before any more can be transferred. As a result, very little energy is available to be distributed among

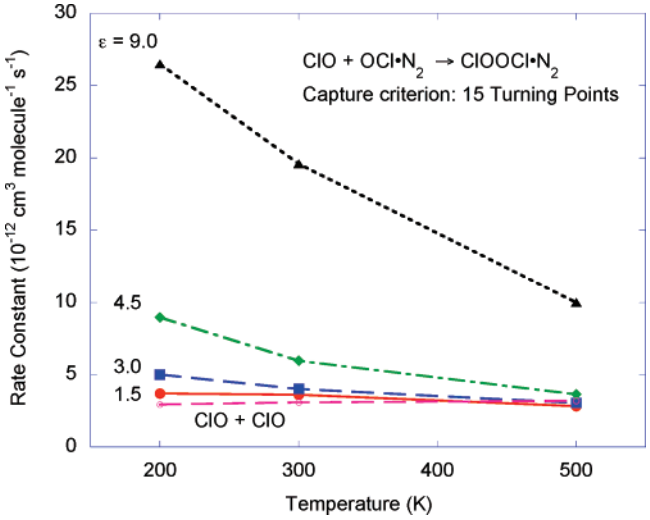

Figure 3. Total capture rate constant k_{cap} as a function of temperature.

the relative degrees of freedom of the recoiling partners; the remainder is retained by the ClOOCl*.

From the trajectory calculations, the total capture rate constant (k_{cap}) corresponding to reaction R10 at the four VDW well depths is shown in Figure 3 as a function of temperature. It is seen that k_{cap} increases as the VDW well depth increases. We surmise that a possible reason for this effect is that as the VDW well depth increases, the VDW stretching and bending modes tend to couple more effectively with the internal modes of ClOOCl. The resulting increased number of modes will result in an increased density of states and an increased lifetime of the nascent ClOOCl*·N_2.

The excited ClOOCl*·N_2 produced in reaction R10 can dissociate via several paths. In the general case, the vibrationally excited VDW complex C*·M (where the excitation resides initially in C, not M) produced in reaction R12 has multiple dissociation channels

$$A{\cdot}M + B \rightarrow C^{*}{\cdot}M \qquad \text{(R12)}$$

$$C^{*}{\cdot}M \rightarrow A{\cdot}M + B \qquad (-\text{R12})$$

$$C^{*}{\cdot}M \rightarrow A + B{\cdot}M \qquad \text{(R13a)}$$

$$C^{*}{\cdot}M \rightarrow C(E) + M \qquad \text{(R13b)}$$

The efficiency of forming C(E) is proportional to the rate of reaction R13b and is given by

$$\xi^{C} = \frac{k_{13b}}{k_{-12} + k_{13a} + k_{13b}} \qquad \text{(E11)}$$

The quasi-classical trajectory calculations show that as the VDW bond becomes stronger, the efficiency decreases substantially. This is because branching via reaction −R12 to regenerate the initial reactants becomes much more important as the VDW bond strength increases. When $\epsilon = 9$ kcal mol^{-1}, the VDW bond strength is comparable to a normal covalent bond. For this case, it is clear that O−O bond redissociation occurs with higher frequency than cleavage of the VDW bond. This result has implications for hydrogen-bonded complexes since hydrogen bonds are usually much stronger than normal VDW bonds.

The overall rate constant $k_{C(E)}$ for forming the vibrationally excited product C(E) depends on both the capture rate constant and the efficiency, $k_{C(E)} = \xi^{C} k_{cap}$. This rate constant (given in

TABLE 5: Rate Constants $k_{C(E)}$ and k_∞ (k_{cap} in Parentheses) for Forming ClOOCl[a]

T(K)	k_∞ for ClO + ClO	$k_{C(E)}$ for ClO + $ClON_2$			
		$\epsilon = 1.5$	$\epsilon = 3.0$	$\epsilon = 4.5$	$\epsilon = 9.0$
200	2.95	3.45 (3.71)[b]	3.11 (5.02)	3.05 (8.97)	2.91 (26.5)
300	3.096 (experiments: 2.0,[c] 1.36 ± 0.22,[d] 3.37 ± 2.67,[e] 4.8 ± 0.5[f])	3.44 (3.62)	3.30 (4.02)	3.35 (5.98)	3.13 (19.6)
500	3.2	2.55 (2.83)	2.63 (3.06)	2.78 (3.66)	2.60 (10.0)

[a] The bimolecular rate constants are in units of 10^{-12} cm^3 molecule^{-1} s^{-1}; the well depth ϵ is in units of kcal mol^{-1} (no ZPE corrections). [b] The values in parentheses correspond to the total capture rate constant k_{cap}. [c] Ref 25. [d] Ref 30. [e] Ref 31. [f] Ref 28.

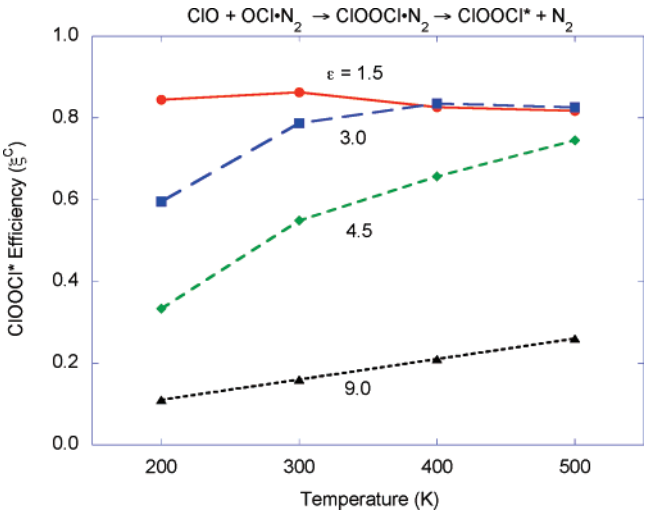

Figure 4. Efficiency of net formation of ClOOCl* as a function of VDW well depth.

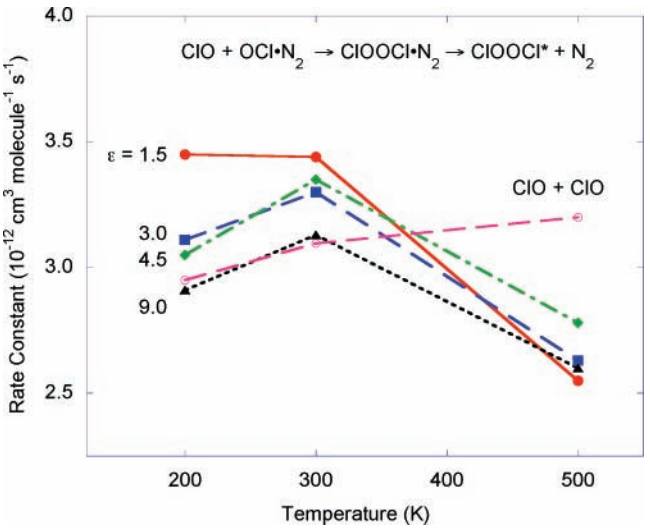

Figure 5. Rate constant for forming ClOOCl*.

Table 5 and Figure 5) is the contribution of the RCM at the high-pressure limit, where every vibrationally excited C(E) is stabilized by collisions. From Figure 5, it is apparent that $k_{C(E)}$ is almost independent of both the well depth and temperature. It is also almost equal to the rate constant (k_∞) for ClO + ClO (in the absence of the RCM) at all three temperatures (the largest deviations are only 10−20%). This result is due to the fortuitous near-cancellation of the temperature dependences of the two factors; the capture rate constant increases at low temperatures, while the efficiency of forming C(E) decreases dramatically. The lack of temperature dependence between 200 and 300 K is at variance with the large effect ($\sim T^{-2.5}$) reported by Stark.[18] The resulting rate constants show that the RCM and the ETM

TABLE 6: Comparison of k_0^c Obtained by RC and ET Mechanisms[a]

	200 K	300 K	500 K
Radical Complex			
VDW ϵ (kcal mol^{-1})	k_0^c	k_0^c	k_0^c
1.5	8.5(−35)	5.3(−35)	3.5(−35)
3.0	3.4(−33)	6.5(−34)	1.7(−34)
4.5	1.5(−31)	8.5(−33)	8.4(−34)
9.0	1.2(−26)	1.5(−29)	7.4(−32)
Energy Transfer[b]	k_0^{scRRKM}	k_0^{scRRKM}	k_0^{scRRKM}
	5.4(−32)	2.4(−32)	8.2(−33)

[a] The ϵ is without ZPE corrections. k_0 notation: 8.5(−35) = 8.5 × 10^{-35} cm^3 molecule^{-1} s^{-1}. [b] Calculated using D_0 = 16.93 kcal mol^{-1}.

are predicted to contribute approximately equally to the overall rate constant for reaction R9 at the high-pressure limit.

The importance of the RCM at the low-pressure limit can also be estimated from the present results. If one assumes that the product C(E) produced by reaction R13b is produced with insufficient energy to dissociate, then an upper limit to the contribution by the RCM to the low-pressure rate constant can be expressed as

$$k_{low}^C \le \xi^C k_{cap} K_{VDW}[M] = k_0^C[M] \qquad \text{(E12)}$$

where $k_0^C = \xi^C k_{cap} K_{VDW}$. Numerical values for k_0^C are given in Table 6. For comparison, low-pressure-limit rate constants (k_0^{scRRKM}) calculated by the MultiWell program[23,24,78] for a strong-collision RRKM model (which is based on the ETM) are also presented in Table 6. The results show that k_0^C is significantly smaller than k_0^{scRRKM} except at the lowest temperatures and greatest well depths investigated. For the VDW well depth obtained at the CCSD(T)//B3LYP level of theory for the ClO + ClO (+N_2) system (ϵ_1 = 1.5 kcal mol^{-1} without ZPE corrections), the RCM is predicted to contribute less than 1% to the total reaction rate at 1 bar of N_2 ($\sim T^{-1.2}$). If K_{VDW} is significantly larger than our estimates, the contribution of the RCM will be larger than this prediction, but we conclude that the RCM (involving N_2) probably plays only a minor role in the overall reaction under atmospheric conditions, despite suggestions to the contrary.[29] This conclusion is in agreement with Stark,[18] although he found a much stronger temperature dependence at the low-pressure limit.

Near the high-pressure limit, the contribution of the RCM to the total rate is given by

$$\frac{\text{RCM}}{\text{RCM} + \text{ET}} = \frac{k_{C(E)} K_{VDW}[N_2]}{k_{C(E)} K_{VDW}[N_2] + k_\infty} \qquad \text{(E13)}$$

where the rate constants were defined earlier and are given in Table 5. At 300 K and 100 bar of N_2 (ϵ_1 = 1.5 kcal mol^{-1}), the contribution of the RCM is ∼4%, which can be compared to

the ~50% estimated by Stark.[18] Although this difference seems large, the present calculations are not necessarily in conflict with Stark's experiments when the possible errors in the calculated well depth, in the calculated equilibrium constant, and in the experimental measurements are considered.

IV. Conclusions

The quasi-classical trajectory calculations described in the preceding sections show that the RCM is potentially more complicated than is usually assumed. First, the capture rate constants are found to increase markedly with decreasing temperature, an effect which has been neglected in the past. Second, the capture complex (ClOOCl*·N_2) may dissociate to give the expected products (ClOOCl* + N_2), but it may also dissociate via the reverse of the formation channel and hence regenerate the reactants (ClO + OCl*·N_2). The net efficiency of forming the recombination product is found to be distinctly temperature-dependent. increasing with increasing temperature. This effect was not anticipated in previous invocations of the RCM. The overall rate constant for forming the recombination product is the product of the capture rate constant and the efficiency. The temperature dependences for these two factors are of opposite sense, and thus, they tend to cancel. In the case of the ClO + ClO·N_2 reaction, the cancellation is fortuitously nearly complete, resulting in an overall rate constant that is nearly independent of temperature.

The nascent energy distribution of the recombination product depends on the VDW well depth, but even small well depths result in enough removal of excitation energy by the VDW partner so that the recombination product does not dissociate significantly, at least for the VDW bond energies considered here. Nonetheless, the recombination product still has considerable excitation and can undergo further reactions if they have lower energy thresholds. This is the case for the ClO + ClO reaction system, for example.[41]

The importance of the RCM depends strongly on K_{VDW}, the equilibrium constant for formation of the radical complex. This equilibrium constant is not the principal focus of the present work, but we show that when the anisotropy of the PES is taken into account, K_{VDW} is nearly 2 orders of magnitude smaller than that when calculated using the isotropic PES assumed in the Bunker−Davidson[9] and Stogryn−Hirschfelder[45] approaches. Order-of-magnitude estimates of K_{VDW} show that it is probably too small for the RCM to play more than a minor role in the ClO + ClO recombination reaction under atmospheric conditions, in agreement with Stark.[18] More accurate quantitative estimates of K_{VDW} can be made by using the Monte Carlo method of Varandas and co-workers,[48−50] which does not require separability of the VDW degrees of freedom.

The radical complex mechanism is important in a number of recombination reaction systems, especially in those containing H_2O, which forms strong hydrogen bonds. Although cumbersome, quasi-classical trajectory methods can provide the information needed for estimates of its importance. The calculated energy distributions can be used to initiate master equation simulations in cases where the RCM is important. Future work will be aimed at developing simpler analytic approximations to make such simulations more practical.

Acknowledgment. Thanks go to Larry Lohr, Phil Stimac, Dave Golden, Juergen Troe, and Andrea Maranzana for helpful discussions. This work was funded, in part, by NASA (Upper Atmosphere Research Program), NASA (Planetary Atmospheres), and NSF (Atmospheric Chemistry Division) under Grant No. 0344102.

References and Notes

(1) Barker, J. R. *J. Phys. Chem.* **1992**, *96*, 7361.
(2) Lindemann, F. A. *Trans. Faraday Soc.* **1922**, *17*, 598.
(3) Troe, J. *Chem. Rev.* **2003**, *103*, 4565.
(4) Forst, W. *Theory of Unimolecular Reactions*; Academic Press: New York, 1973.
(5) Forst, W. *Unimolecular Reactions. A Concise Introduction*; Cambridge University Press: Cambridge, U. K., 2003.
(6) Gilbert, R. G.; Smith, S. C. *Theory of Unimolecular and Recombination Reactions*; Blackwell Scientific: Oxford, U. K., 1990.
(7) Holbrook, K. A.; Pilling, M. J.; Robertson, S. H. *Unimolecular Reactions*, 2 ed.; Wiley: Chichester, U. K., 1996.
(8) Robinson, P. J.; Holbrook, K. A. *Unimolecular Reactions*; Wiley-Interscience: New York, 1972.
(9) Bunker, D. L.; Davidson, N. *J. Am. Chem. Soc* **1958**, *80*, 5090.
(10) Lii, R.-R.; Sauer, M. C. J.; Gordon, S. *J. Phys. Chem.* **1981**, *85*, 2833.
(11) Kircher, C. C.; Sander, S. P. *J. Phys. Chem.* **1984**, *88*, 2082.
(12) Sander, S. P.; Friedl, R. R.; Ravishankara, A. R.; Golden, D. M.; Kolb, C. E.; Kurylo, M. J.; Huie, R. E.; Orkin, V. L.; Molina, M. J.; Moortgat, G. K.; Finlayson-Pitts, J. B. *Chemical Kinetics and Photochemical Data for Use in Stratospheric Modeling*, Evaluation Number 14; Jet Propulsion Laboratory: Pasadena, CA, 2003; http://jpldataeval.jpl.nasa.gov/.
(13) Aloisio, S.; Francisco, J. S.; Friedl, R. R. *J. Phys. Chem. A* **2000**, *104*, 6597.
(14) Zhu, R. S.; Lin, M. C. *Phys. Chem. Commun.* **2001**, *4*, 106.
(15) Zhu, R. S.; Xu, Z. F.; Lin, M. C. *J. Chem. Phys.* **2002**, *116*, 7452.
(16) Luther, K.; Oum, K.; Troe, J. *J. Phys. Chem. A* **2001**, *105*, 5535.
(17) Luther, K.; Oum, K.; Troe, J. *Phys. Chem. Chem. Phys.* **2005**, *7*, 2764.
(18) Stark, H. Druckabhängigkeit, Temperaturabhängigkeit und Einfluss des Komplex-mechanismus bei der Rekombination von CIO-molekülen [3-89712-607-9]. Ph. D., University of Göttingen, Germany, 1999.
(19) Hippler, H.; Rahn, R.; Troe, J. *J. Chem. Phys.* **1990**, *93*, 6560.
(20) Oum, K.; Luther, K.; Troe, J. *J. Phys. Chem. A* **2004**, *108*, 2690.
(21) Atkinson, R.; Baulch, D. L.; Cox, R. A.; Crowley, J.; Hampson, R. F.; Jenkin, M. E.; Kerr, J. A.; Rossi, M. J.; Troe, J. *Evaluated Kinetic Data*; IUPAC Subcommittee for Gas Kinetic Data Evaluation for Atmospheric Chemistry: Cambridge, U.K., 2002; http://www.iupac-kinetic.ch-.cam.ac.uk/index.html.
(22) Barker, J. R.; Golden, D. M. *Chem. Rev.* **2003**, *103*, 4577.
(23) Barker, J. R. *Int. J. Chem. Kinet.* **2001**, *33*, 232.
(24) Barker, J. R.; Ortiz, N. F.; Preses, J. M.; Lohr, L. L.; Maranzana, A.; Stimac, P. J. *MultiWell-2.08 Software*; University of Michigan: Ann Arbor, MI, 2007.
(25) Golden, D. M. *Int. J. Chem. Kinet.* **2003**, *35*, 206.
(26) Cox, R. A.; Hayman, G. D. *Nature* **1988**, *332*, 796.
(27) Sander, S. P.; Friedl, R. R.; Yung, Y. L. *Science* **1989**, *145*, 1095.
(28) Trolier, M.; Mauldin, R. L., III; Ravishankara, A. R. *J. Phys. Chem.* **1990**, *94*, 4896.
(29) Nickolaisen, S. L.; Friedl, R. R.; Sander, S. P. *J. Phys. Chem.* **1994**, *98*, 155.
(30) Bloss, W. J.; Nickolaisen, S. L.; Salawich, R. J.; Friedl, R. R.; Sander, S. P. *J. Phys. Chem. A* **2001**, *105*, 11226.
(31) Boakes, G.; Mok, W. H. H.; Rowley, D. M. *Phys. Chem. Chem. Phys.* **2005**, *7*, 4102.
(32) Christen, D.; Mack, H. G.; Muller, H. S. P. *J. Mol. Struct.* **1999**, *509*, 137.
(33) Jensen, F.; Oddershede, J. *J. Phys. Chem.* **1990**, *94*, 2235.
(34) Lee, T. J.; Rohlfing, C. M.; Rice, J. E. *J. Chem. Phys.* **1992**, *97*, 6593.
(35) McGrath, M. P.; Francl, M. M.; Rowland, F. S.; Hehre, W. J. *J. Phys. Chem.* **1988**, *92*, 5352.
(36) McGrath, M. P.; Clemitshaw, K. C.; Rowlandand, F. S.; Hehre, W. J. *J. Phys. Chem.* **1990**, *94*, 6126.
(37) Rendell, A. P.; Lee, T. J. *J. Chem. Phys.* **1991**, *94*, 6219.
(38) Slanina, Z.; Uhlik, F. *J. Phys. Chem.* **1991**, *95*, 5432.
(39) Slanina, Z.; Uhlik, F. *Chem. Phys. Lett.* **1991**, *182*, 51.
(40) Stanton, J. F.; Magnus, C.; Rittby, L.; Bartlett, R. J.; Toohey, D. W. *J. Phys. Chem.* **1991**, *95*, 2107.
(41) Zhu, R. S.; Lin, M. C. *J. Chem. Phys.* **2003**, *118*, 4094.
(42) Francisco, J. S.; Sander, S. P. *J. Am. Chem. Soc* **1995**, *117*, 9917.
(43) Vogel, B.; Feng, W.; Streibel, M.; Müller, R. *Atmos. Chem. Phys.* **2006**, *6*, 3099.
(44) Atkinson, R.; Baulch, D. L.; Cox, R. A.; Crowley, J.; Hampson, R. F.; Hynes, R. G.; Jenkin, M. E.; Rossi, M. J.; Troe, J. *Atmos. Chem. Phys.* **2007**, *7*, 981.
(45) Stogryn, D. E.; Hirschfelder, J. O. *J. Chem. Phys.* **1959**, *31*, 1531.
(46) Schwarzer, D.; Teubner, M. *J. Chem. Phys.* **2002**, *116*, 5680.
(47) Dardi, P. S.; Dahler, J. S. *J. Chem. Phys.* **1990**, *93*, 3562.
(48) Urbano, A. P. A.; Prudente, F. V.; Riganelli, A.; Varandas, A. J. C. *Phys. Chem. Chem. Phys.* **2001**, *3*, 5000.

(49) Riganelli, A.; Varandas, A. J. C. *J. Phys. Chem. A* **1999**, *103*, 8303.
(50) Prudente, F. V.; Riganelli, A.; Varandas, A. J. C. *J. Phys. Chem. A* **2001**, *105*, 5272.
(51) Varandas, A. J. C.; Pais, A. A. C. C.; Marques, J. M. C.; Wang, W. *Chem. Phys. Lett.* **1996**, *249*, 264.
(52) Frisch, M. J.; Trucks, G. W.; Schlegel, H. B.; Scuseria, G. E.; Robb, M. A.; Cheeseman, J. R.; Zakrzewski, V. G.; Montgomery, J. A., Jr.; Stratmann, R. E.; Burant, J. C.; Dapprich, S.; Millam, J. M.; Daniels, A. D.; Kudin, K. N.; Strain, M. C.; Farkas, O.; Tomasi, J.; Barone, V.; Cossi, M.; Cammi, R.; Mennucci, B.; Pomelli, C.; Adamo, C.; Clifford, S.; Ochterski, J.; Petersson, G. A.; Ayala, P. Y.; Cui, Q.; Morokuma, K.; Malick, D. K.; Rabuck, A. D.; Raghavachari, K.; Foresman, J. B.; Cioslowski, J.; Ortiz, J. V.; Stefanov, B. B.; Liu, G.; Liashenko, A.; Piskorz, P.; Komaromi, I.; Gomperts, R.; Martin, R. L.; Fox, D. J.; Keith, T.; Al-Laham, M. A.; Peng, C. Y.; Nanayakkara, A.; Gonzalez, C.; Challacombe, M.; Gill, P. M. W.; Johnson, B. G.; Chen, W.; Wong, M. W.; Andres, J. L.; Head-Gordon, M.; Replogle, E. S.; Pople, J. A. *Gaussian 98*, revision A.7; Gaussian, Inc.: Pittsburgh, PA, 1998.
(53) Hase, W. L.; Duchovic, R. J.; Hu, X.; Komornicki, A.; Lim, K. F.; Lu, D.-H.; Peslherbe, G. H.; Swamy, K. N.; Linde, S. R. V.; Varandas, A.; Wang, H.; Wolf, R. J. *Quantum Chem. Program Exchange Bull.* **1996**, *16*, 43.
(54) Lu, D. H.; Hase, W. L.; Wolf, R. J. *J. Chem. Phys.* **1986**, *85*, 4422.
(55) Becke, A. D. *J. Chem. Phys.* **1993**, *98*, 5648.
(56) Lee, C.; Yang, W.; Parr, R. G. *Phys. Rev. B* **1988**, *37*, 785.
(57) Curtiss, L. A.; Redfern, P. C.; Raghavachari, K.; Rassolov, V.; Pople, J. A. *J. Chem. Phys.* **1999**, *110*, 4703.
(58) *Monte Carlo Sampling for Classical Trajectory Simulations*; Peslherbe, G. H., Wang, H., Hase, W. L., Eds.; Wiley: New York, 1999; Vol. 105, pp 171−201.
(59) Liu, Y.; Lohr, L. L.; Barker, J. R. *J. Phys. Chem. A* **2006**, *110*, 1267.
(60) Chase, M. W., Jr. *J. Phys. Chem. Ref. Data* **1998**, *Monograph No. 9*, 1.
(61) Yoder, L. M.; Barker, J. R. *J. Phys. Chem. A* **2000**, *104*, 10184.
(62) Stimac, P. J.; Barker, J. R. *J. Phys. Chem. A* **2006**, *110*, 6851.
(63) Liu, Y.; Lohr, L. L.; Barker, J. R. *J. Phys. Chem. B* **2005**, *109*, 8304.
(64) Plenge, J.; Kuhl, S.; Vogel, B.; Muller, R.; Stroh, F.; von Hobe, M.; Flesch, R.; Ruhl, E. *J. Phys. Chem. A* **2005**, *109*, 6730.
(65) Bröske, R.; Zabel, F. *J. Phys. Chem. A* **2006**, *110*, 3280.
(66) Boys, S. F.; Bernardi, F. *Mol. Phys.* **1970**, *19*, 553.
(67) Montgomery, J. A.; Frisch, M. J.; Ochterski, J. W.; Petersson, G. A. *J. Chem. Phys.* **1999**, *110*, 2822.
(68) Montgomery, J. A.; Frisch, M. J.; Ochterski, J. W.; Petersson, G. A. *J. Chem. Phys.* **2000**, *112*, 6532.
(69) Dunning, T. H. *J. Phys. Chem. A* **2000**, *104*, 9062.
(70) Hunt, S. W.; Leopold, K. R. *J. Phys. Chem. A* **2001**, *105*, 5498.
(71) Valdes, H.; Sordo, J. A. *J. Phys. Chem. A* **2002**, *106*, 3690.
(72) Valdes, H.; Sordo, J. A. *J. Comput. Chem.* **2002**, *23*, 444.
(73) Galano, A.; Alvarez-Idaboy, J. R.; Ruiz-Santoyo, M. E.; Vivier-Bunge, A. *ChemPhysChem* **2004**, *5*, 1379.
(74) Luther, K.; Oum, K.; Sekiguchi, K.; Troe, J. *Phys. Chem. Chem. Phys.* **2004**, *6*, 4133.
(75) Yoder, L. M.; Barker, J. R. *Phys. Chem. Chem. Phys.* **2000**, *2*, 813.
(76) Yoder, L. M.; Barker, J. R.; Lorenz, K. T.; Chandler, D. W. *Chem. Phys. Lett.* **1999**, *302*, 602.
(77) Yoder, L. M.; Barker, J. R.; Lorenz, K. T.; Chandler, D. W. Recoil Energy Distributions in van der Waals Cluster Vibrational Predissociation. In *Imaging in Chemical Dynamics*; Suits, A. G., Continetti, R. E., Eds.; American Chemical Society: Washington, DC, 2000; Vol. 770, pp 151−166.
(78) Barker, J. R.; Ortiz, N. F.; Preses, J. M.; Lohr, L. L.; Maranzana, A.; Stimac, P. J. *MultiWell-2.03 Software*; University of Michigan: Ann Arbor, MI, 2006.
(79) Jacobs, J.; Kronberg, M.; Muller, H. S. P.; Willner, H. *J. Am. Chem. Soc* **1994**, *116*, 1106.